Article

Cell Reports

Oxidative Homeostasis Regulates the Response to Reductive Endoplasmic Reticulum Stress through Translation Control

Graphical Abstract

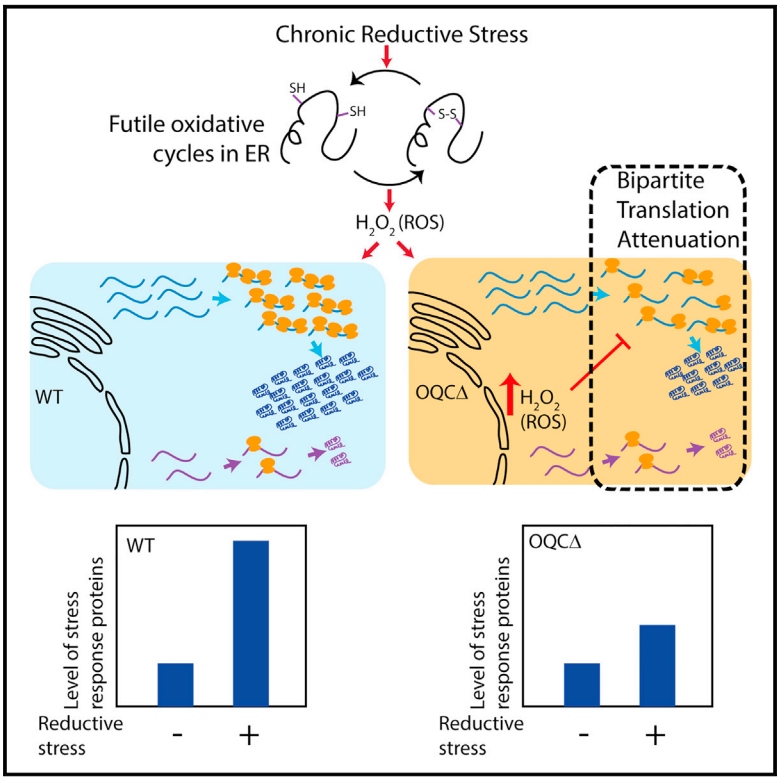

Authors

Shuvadeep Maity, Asher Rajkumar, Latika Matai, ..., Arnab Mukhopadhyay, Shantanu Sengupta, Kausik Chakraborty

Correspondence

kausik@igib.res.in

In Brief

Maity et al. show that oxidative stress plays an important role in controlling the cellular response to ER stress. They show that this happens through a non-canonical translation regulation by reactive oxygen species that decrease the level of abundant proteins and increase the level of non-abundant ones.

Highlights

- Oxidative quality control pathways are essential to counteract reductive ER stress
- Failure of oxidative quality leads to accumulation of peroxide during ER stress
- Non-canonical bimodal translation regulation by peroxide blocks the ER stress response
- This is prevented by activation of canonical PERK-dependent translation regulation

Accession Numbers

GSE68006

Maity et al., 2016, Cell Reports *16*, 851–865
July 19, 2016
http://dx.doi.org/10.1016/j.celrep.2016.06.025

Cell Reports
Article

Oxidative Homeostasis Regulates the Response to Reductive Endoplasmic Reticulum Stress through Translation Control

Shuvadeep Maity,[1,4] Asher Rajkumar,[1,3,4] Latika Matai,[1,3,4] Ajay Bhat,[1,3] Asmita Ghosh,[1,3] Ganesh Agam,[1] Simarjot Kaur,[1] Niraj R. Bhatt,[1,3] Arnab Mukhopadhyay,[2,5] Shantanu Sengupta,[1,3,5] and Kausik Chakraborty[1,3,5,*]
[1]CSIR-Institute of Genomics and Integrative Biology, South Campus, Mathura Road, New Delhi 110025, India
[2]Molecular Aging Laboratory, National Institute of Immunology, New Delhi 110067, India
[3]Academy of Scientific and Innovative Research, CSIR- Institute of Genomics and Integrative Biology, Mathura Road Campus, New Delhi 110025, India
[4]Co-first author
[5]Co-senior author
*Correspondence: kausik@igib.res.in
http://dx.doi.org/10.1016/j.celrep.2016.06.025

SUMMARY

Reductive stress leads to the loss of disulfide bond formation and induces the unfolded protein response of the endoplasmic reticulum (UPR^{ER}), necessary to regain proteostasis in the compartment. Here we show that peroxide accumulation during reductive stress attenuates UPR^{ER} amplitude by altering translation without any discernible effect on transcription. Through a comprehensive genetic screen in *Saccharomyces cerevisiae*, we identify modulators of reductive stress-induced UPR^{ER} and demonstrate that oxidative quality control (OQC) genes modulate this cellular response in the presence of chronic but not acute reductive stress. Using a combination of microarray and relative quantitative proteomics, we uncover a non-canonical translation attenuation mechanism that acts in a bipartite manner to selectively downregulate highly expressed proteins, decoupling the cell's transcriptional and translational response during reductive ER stress. Finally, we demonstrate that PERK, a canonical translation attenuator in higher eukaryotes, helps in bypassing a ROS-dependent, non-canonical mode of translation attenuation.

INTRODUCTION

Cells respond to environmental stress by upregulating stress- and compartment-specific response pathways. Thus, genetic or epigenetic predispositions that prevent cells from mounting an effective stress response lead to compromised stress tolerance. One of the stress response pathways, unfolded protein response of the endoplasmic reticulum (unfolded protein response element [UPR]^{ER}), is responsible for maintaining ER homeostasis during ER stress (Cao and Kaufman, 2012; Ron and Walter, 2007; Walter and Ron, 2011). UPR^{ER} plays a crucial role in ensuring proper folding of the membrane and secretory proteins in this compartment during conditions that lead to protein misfolding (Mori et al., 1992), thereby restoring ER homeostasis (Walter and Ron, 2011). Protein folding in the ER may be compromised either because of a decrease in glycosylation activity or a reduction in disulfide-mediated folding (reductive stress). The latter is of immediate interest because secretory cells, like pancreatic acinar cells, are burdened with a large load of disulfide-bonded proteomes. Because a high disulfide load mimics reductive ER stress, it is important to decipher the regulators of reductive stress-induced UPR^{ER} to identify genetic modules that play a crucial role in maintaining ER homeostasis in these tissues. A loss of ER homeostasis or unusually high UPR^{ER} is closely associated with multiple complex disorders, including type II diabetes and cardiovascular diseases (Back and Kaufman, 2012; Malhotra and Kaufman, 2007). Importantly, with progressing age, the ability of an organism to mount an effective response to ER stress declines significantly (Taylor and Dillin, 2013), and this explains the manifestation of late-onset complex disorders. However, the reason for this decline is still an unanswered question.

UPR^{ER} requires the coordinate function of IRE-1/IRE1(Tirasophon et al., 1998), PEK-1/PERK (Harding et al., 2000), and ATF-6/ATF6 (Haze et al., 1999) in nematodes and higher eukaryotes, respectively, whereas, in the unicellular eukaryote *Saccharomyces cerevisiae*, Ire1 (Shamu and Walter, 1996) is the sole sensor. Genetic modulators of basal UPR^{ER} (bUPR^{ER}) were initially characterized as the functional module to maintain ER homeostasis (Jonikas et al., 2009). However, how different genes regulate the Ire1 branch of UPR^{ER} under stress is unknown. Because any integrative stress response acts as a combination of multiple cellular processes, a genetic deletion that is sensitive to ER stress may not necessarily be defective in mounting UPR^{ER}. On the other hand, deletions that already induce a mild ER stress may aggravate sensitivity to additional stressors without altering the cellular capacity to respond (Jonikas et al., 2009). Thus, modulators of basal UPR^{ER} may not be essential for mounting UPR^{ER} under stress conditions. This phenomenon has been reported for the cytosolic UPR (Brandman et al., 2012).

To uncover the role of genetic UPR^{ER} modulators and their crosstalk with other physiological processes during reductive stress, we used a combination of a yeast genetic screen, microarray, quantitative proteomics, and targeted genetic approach. We next asked whether these regulators are conserved in higher eukaryotes that have evolved multiple branches of the UPR^{ER}. Finally, we wished to delineate whether these regulators play a role during age-associated decline in UPR^{ER}. We identified the genes that are involved in the maintenance of homeostasis during oxidative stress, called oxidative quality control (OQC) genes hereafter, to be the major regulators of reductive stress-induced UPR^{ER} (red-iUPR^{ER}). Interestingly, yeast OQC was essential for regulation of UPR^{ER} only during a chronic stress and not during an acute one. We unraveled that reactive oxygen species (ROS) muffled UPR^{ER} by downregulating translation during reductive ER stress in a bipartite manner—a previously unknown aspect of translation control. We found this mechanism to be conserved in *Caenorhabditis elegans* harboring multiple UPR^{ER} branches. We show that ROS from different sources may negatively regulate UPR^{ER} and that this regulation can partially explain aging-associated loss of UPR^{ER}. Interestingly, the PERK-mediated translation attenuation pathway is required to prevent ROS-dependent deregulation of translation during UPR^{ER}. Because oxidative folding results in ROS formation, we speculate that evolution of the PERK branch of UPR^{ER} may have facilitated the emergence of high disulfide-rich proteomes in higher eukaryotes.

RESULTS

A Comprehensive Genetic Screen Identifies Modulators of Reductive Stress-Induced UPR^{ER}

To identify the modulators of iUPR^{ER}, we used a reporter strain of *S. cerevisiae* expressing GFP under the control of a UPR^{ER}-inducible synthetic promoter and mCherry driven by the constitutive promoter of *tef2* (Jonikas et al., 2009). Induction of UPR^{ER} was followed by the corresponding increase in GFP fluorescence while the fluorescence of mCherry was used to monitor the basal level of transcription and translation (Figure 1A). GFP induction showed a dose-dependent response to DTT, making this assay a quantitative readout for red-iUPR^{ER} (Jonikas et al., 2009; Figure 1A). Using a commercially available *S. cerevisiae* deletion library of ~4,500 non-essential genes (Winzeler et al., 1999) and a hypomorph library of ~800 essential genes (Breslow et al., 2008) (referred to collectively as deletion strains, Openbiosystems), we introduced the reporter into each of the deletion strains using a synthetic genetic array technique (Tong et al., 2001). To identify genes that interact with or modulate the amplitude of red-iUPR^{ER}, these strains were grown in the presence or absence of DTT, and the amplitude of red-iUPR^{ER} or bUPR^{ER} (in the absence of DTT) was quantified by single-cell fluorescence analysis using flow cytometry. Comprehensive screening of the deletion strains revealed that a large number of genes modulate the amplitude of red-iUPR^{ER} (see Figure 1B, Figure S1A, and Table S1 for full details). To elucidate the dominant mechanisms of red-iUPR^{ER} modulation, we selected 121 candidate genes whose deletion results in a significant reduction of DTT-induced UPR^{ER} using a stringent cutoff (Z score < -4 for GFP and > -2.0 for RFP upon DTT treatment). The RFP cutoff was used to exclude strains that had a constitutive decrease in transcriptional and translational capacity. Although this is a conservative approach to identify strong modifiers, this stringent cutoff may have led to the omission of genes that are potentially involved in regulating iUPR^{ER} as well as translation/transcription machineries. As expected, *hac1*, *yfl032w* (a dubious open reading frame that overlaps with *hac1*) and *tpt1* (an essential enzyme required for the final step of *hac1* splicing) (Schwer et al., 2004) were found to be strong positive modulators of red-iUPR^{ER} (Figure 1B). Furthermore, many of the earlier reported genes (Rand and Grant, 2006) were also identified, providing confidence that the other candidates may indeed be responsible for iUPR^{ER} regulation.

Our results indicate that genes involved in maintaining red-iUPR^{ER} minimally overlapped with the genes that are either overexpressed during ER stress (Travers et al., 2000; Figure S1B; p value, 0.99) or those involved in maintaining ER homeostasis (Jonikas et al., 2009; Figure S1B; p value, 0.74). Moreover, bUPR^{ER} was not a predictor of the amplitude of red-iUPR^{ER} (Figure 1C), indicating that the genetic modules involved in the control of ER homeostasis and the ones involved in the control of cellular response to ER stress may be mechanistically distinct. Furthermore, a large number of gene products involved in red-iUPR^{ER} modulation are localized in cellular compartments other than the ER (Figure 1D). Although a large number (53 of 121) of the positive regulators of red-iUPR^{ER} localized to the cytosol, there was a minimal overlap with the positive modulators of cytosolic iUPR, the heat shock response (HSR) (Brandman et al., 2012; Figure S1C; p value, 0.75). These observations suggest that distinct molecular players regulate stress response pathways in different cellular compartments.

Oxidative Stress Response Pathways Are Important for Maintaining iUPR^{ER} Amplitude in Yeast

Subsequently, we focused on the non-essential candidates and regenerated the strains by re-crossing the reporter into the deletion strains. Finally, 22 deletion strains that exhibited consistent downregulation of red-iUPR^{ER} without any significant effect on RFP expression were selected for further study (refer to the Supplemental Experimental Procedures for details on hit selection, Figures S1D, S1E, and S1F in the Supplemental Experimental Procedures, and Tables S5 and Table S6). Interestingly, *skn7Δ*, *yap1Δ,* and *hyr1Δ*, all known to play a role in the cellular OQC pathway (Avery and Avery, 2001; Temple et al., 2005), were found to modulate the response to reductive stress. We chose this cluster to delineate the mechanism of red-iUPR^{ER} modulation because these genes are also known to be required for ER stress tolerance (Rand and Grant, 2006). The other strains were not selected as these, with the exception of *hac1Δ* and *yfl032wΔ*, showed a conditional loss of red-UPR^{ER} only in the presence of G418 (Figure S1F in the Supplemental Experimental Procedures). It is important to note that strains that have altered GFP fluorophore maturation may also appear as hits in the screen. Validation of altered GFP expression at the protein level or mRNA level is thus important to confirm the importance of the hits in modulating iUPR^{ER}. We experimentally validated the deletion strains and their GFP expression (Supplemental

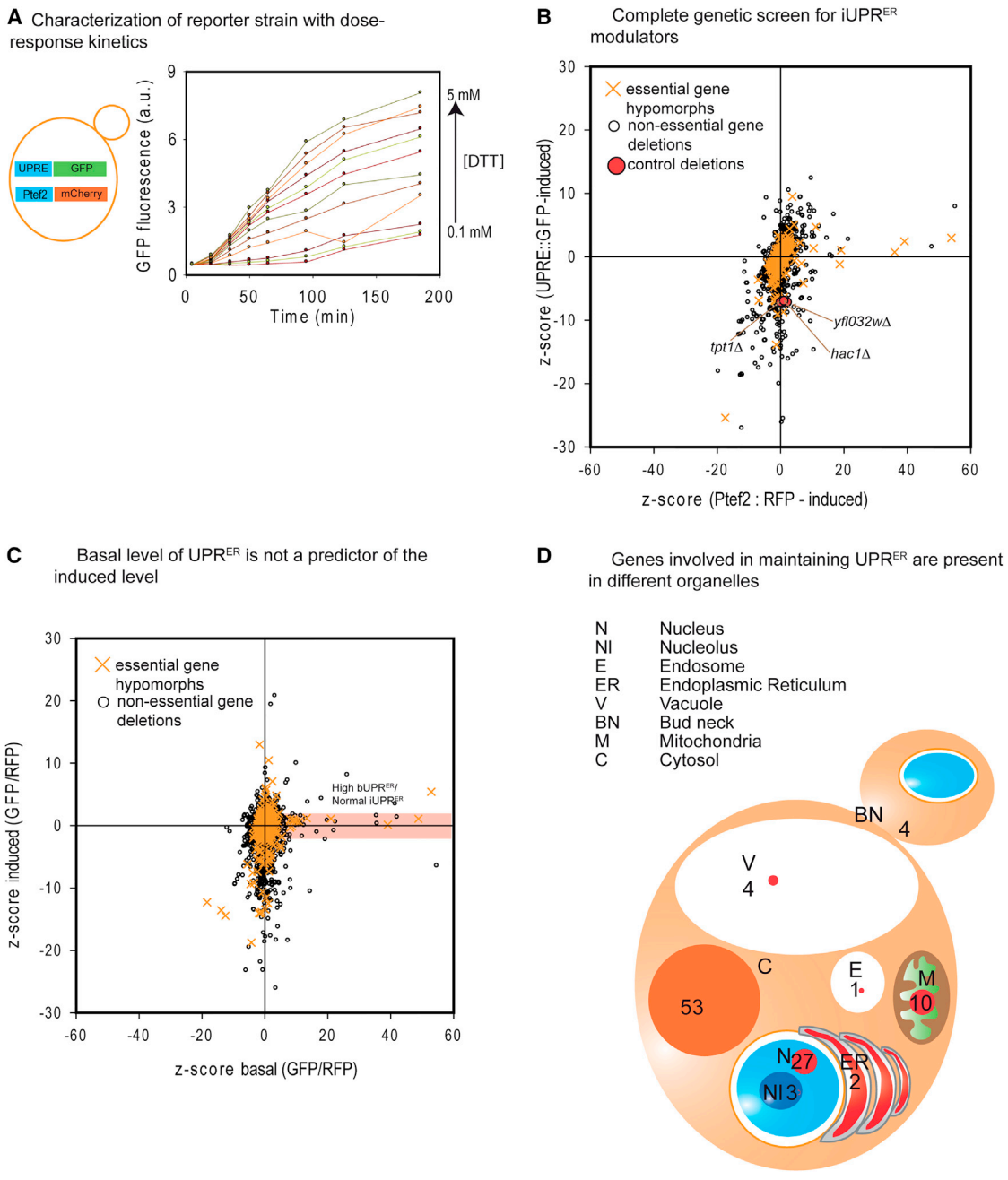

Figure 1. A Comprehensive Genetic Screen to Identify UPR^{ER} Modulators in *S. cerevisiae*

(A) The reporter strain used has a *gfp* driven by a UPRE-containing synthetic promoter and an *rfp* under the control of a UPR-independent promoter of *tef2*. The dose response of the strain on different concentrations of DTT (0.1–5 mM) was tracked over 3 hr.

(B) Results of the genetic screen with the *Z* scores of UPRE-GFP and P*tef2*-RFP on the y and x axis, respectively. Each point represents a loss-of-function strain. The control deletions are shown as red dots.

(C) *Z* scores for bUPR^{ER} are plotted on the x axis and the *Z* scores for iUPR^{ER} on the y axis for each of the strains. The red region indicates strains exhibiting high bUPR^{ER} but normal iUPR^{ER}.

(D) The number of positive candidates that localized to the different cellular compartments.

See also Supplemental Notes, Figure S1, and Table S1.

Notes; Figures S2A–S2C), thereby establishing that the OQC genes are bona fide modulators of the amplitude of red-iUPR^{ER} and not GFP maturation.

Because *yap1* and *skn7* are known to be involved in the oxidative stress response (Lee et al., 1999), we monitored ROS using superoxide anion-specific (dihydroethidium or DHE) (Tarpey and

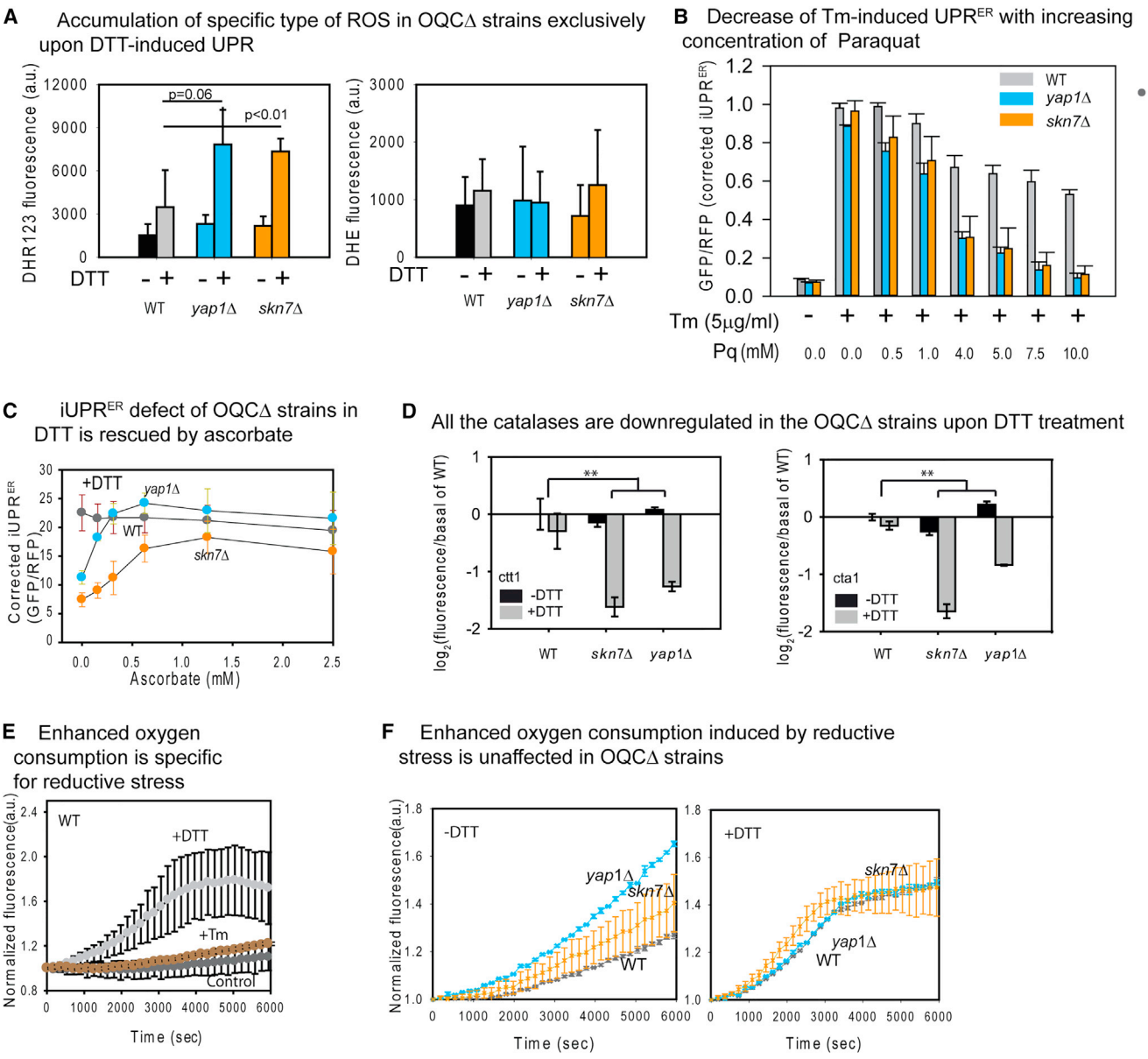

Figure 2. OQC Genes Reduce ROS Accumulation during Reductive ER Stress

(A) Accumulation of ROS measured using dyes that specifically detect superoxide anion (DHE, right) or peroxide (DHR123, left). The different strains, untreated or treated with 5 mM DTT for 180 min, were stained with the indicated dyes, and median fluorescence was recorded using flow cytometry.

(B) WT and OQCΔ strains were simultaneously treated with Tm (5 μg/ml) and different concentrations of Pq. iUPR^{ER} was monitored using flow cytometry after 4 hr of treatment.

(C) WT and OQCΔ strains were grown in different concentrations of ascorbate and then treated with DTT. iUPR^{ER} was measured as above.

(D) Comparative level of catalase transcripts of the OQCΔ and WT strains upon DTT treatment as monitored by microarray.

(E) Oxygen consumption was monitored using an Oxyplate assay in WT cells with or without DTT (5 mM) or Tm (10 μg/ml). An increase in fluorescence is indicative of enhanced oxygen consumption.

(F) The Oxyplate assay was performed for WT and OQCΔ strains in the absence (left) and presence of 5 mM DTT (right).

For all samples, *p < 0.1, **p < 0.05, and ***p < 0.01 with a minimum of three replicates. See also Supplemental Notes for this figure, Figure S2, and Table S2.

Fridovich, 2001) and peroxide-specific (dihydrorhodamine 123 or DHR123) (Henderson and Chappell, 1993) fluorescent dyes. We observed significantly higher DHR123 fluorescence in OQCΔ strains upon reductive stress compared with the wild-type (WT) (Figure 2A, left), whereas DHE did not show any significant difference (Figure 2A, right). This points to the accumulation of peroxide during reductive stress. A number of targeted tests confirmed that the decrease in the amplitude of red-iUPR^{ER} is

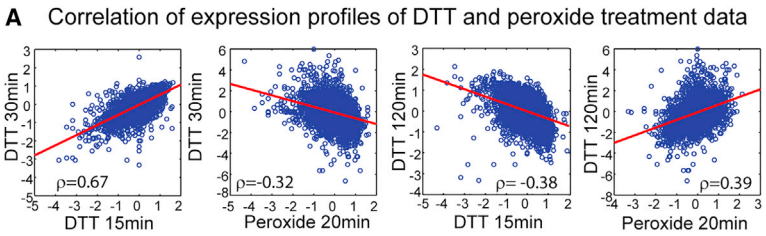

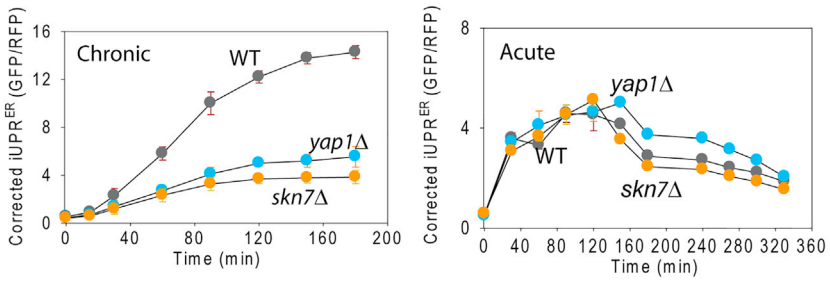

Figure 3. Formation of ROS during Reductive UPR^{ER} Is a Slow Phenomenon and Is Unaffected in OQCΔ Strains

(A) Meta-analysis of previously reported gene expression data (Gasch et al., 2000).

(B) iUPR^{ER} was monitored in WT and OQCΔ strains on continuous treatment with 5 mM DTT (left) or upon a 30-min treatment with 5 mM DTT followed by DTT removal (right).

due to the accumulation of a ROS (peroxide). First, addition of tunicamycin (Tm), an ER stressor that acts by blocking N-linked glycosylation, to OQCΔ strains resulted in only a marginal decrease in iUPR^{ER} with respect to the WT (Figure S2D, left and center) and accumulation of significantly lower amounts of peroxide in the OQCΔ strains (Figure S2E). However, another reducing agent, β-mercaptoethanol, exhibited an effect that was similar to DTT (Figure S2D, right). Second, exogenous addition of peroxide resulted in a dose-dependent reduction of Tm-iUPR^{ER} in the WT and, at a much lower concentration of peroxide, in OQCΔ strains (Figure S2F). Similarly, paraquat (Pq), a peroxide generator, suppressed Tm-iUPR^{ER} in both WT and OQCΔ strains (Figure 2B), whereas menadione, a superoxide generator, did not alter the response (Figure S2G). Third, exogenous addition of ascorbate, a potent ROS scavenger, alleviated the low red-iUPR^{ER} of OQCΔ strains (Figure 2C), rendering mutants more resistant to DTT than the untreated ones (Figures S2H and S2I). Thus, supplementation of a ROS-scavenging agent in OQCΔ strains restores the WT phenotype. These experiments support the association of peroxide accumulation with reductive stress and underscore the importance of the canonical anti-oxidative function of OQC genes in maintaining red-iUPR^{ER} and conferring tolerance to reductive stress.

We performed unbiased transcriptome profiling of the candidate mutants and found that catalases required for scavenging peroxides were significantly downregulated upon DTT treatment in the OQCΔ strains compared with the WT (Figure 2D; Figure S2J; Table S2). This hinted at the possibility that the ROS-scavenging mechanisms of OQCΔ strains may be impaired, leading to increased ROS accumulation during reductive stress. Because oxygen consumption is required for ROS formation, using a fluorescence-based oxygen consumption assay (Oxyplate), we observed enhanced oxygen consumption in WT and OQCΔ strains upon DTT treatment (Figures 2E and 2F) but not with Tm. This was consistent with ROS formation during reductive stress. However, there was no difference between WT and OQCΔ strains (Figure 2F, right; see details in the Supplemental Notes), ruling out any difference in ROS production, further proving that ROS clearance defects enhance the ROS-dependent UPR^{ER} decrease in OQCΔ strains during reductive stress.

Thus, defects in the ROS-scavenging pathways during reductive ER stress lead to accumulation of ROS that decrease the amplitude of iUPR^{ER} during reductive stress in yeast.

ROS Accumulation Acts as a State Sensor that Distinguishes Chronic from Acute Stress

If the ROS clearance mechanism is crucial for the iUPR^{ER}, then we hypothesized that the effect could be a late-phase response during chronic insult. Indeed, meta-analysis of previously published time kinetics microarray data for DTT and peroxide treatment (Gasch et al., 2000) revealed that the expression profiles during early points of DTT treatment are anti-correlative with the late time points (Figure 3A). This suggested that a different transcriptional program may be activated at the later stages. Only the late-phase reductive stress-induced gene expression profiles correlate strongly with that of early-stage peroxide stress (Figure 3A). This suggested a ROS-activated switch in transcription profile during late stages of reductive ER stress. If the ROS accumulates slowly during a reductive insult and acts only during the later phases of the reductive stress response, an acute pulse of DTT should not lead to ROS-dependent abrogation of red-iUPR^{ER}. Hence, the red-iUPR^{ER} observed with this treatment regime should be independent of the ROS-scavenging mechanisms. Indeed, the OQCΔ strains that showed a drastic reduction of red-iUPR^{ER} during chronic reductive stress (Figure 3B, left), exhibited only marginal differences compared with the WT strain when responding to an acute reductive stress (Figure 3B, right). Together, these observations suggest that ROS accumulation during chronic reductive stress initiates the oxidative stress response. In the absence of a functional oxidative response, ROS accumulation abrogates the cellular response to reductive ER stress.

Failure of Oxidative Quality Control Shuts Off Translation in Yeast

Toward investigating the mechanism by which UPR^{ER} is blocked in the presence of unresolved oxidative stress, we monitored the

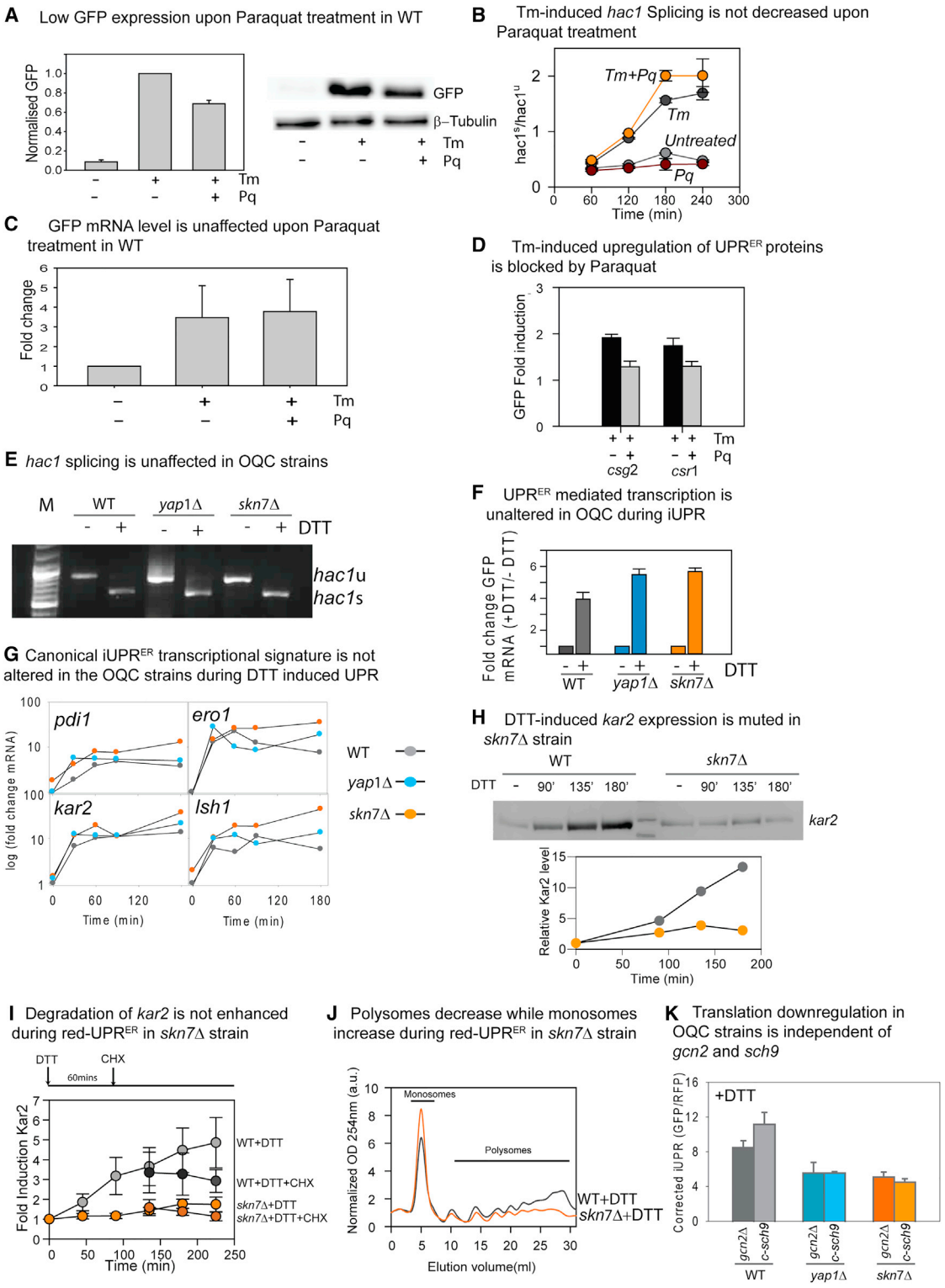

Figure 4. Failure of OQC Leads to Downregulation of iUPR^{ER} at the Level of Translation

(A) Immunoblot for GFP in the WT treated with Tm in the presence or absence of Pq. Left: quantitated graph for three independent experiments normalized to tubulin.

(B) *Hac1* splicing in the WT measured by semiquantitative PCR upon treatment with Tm in the presence or absence of Pq.

(C) *gfp* transcript levels upon Tm treatment in the presence or absence of Pq were monitored with qRT-PCR in the WT.

(legend continued on next page)

effect of Pq on Tm-iUPR^{ER}. Addition of Pq led to the downregulation of GFP at the protein level (Figure 4A); however, Hac1 splicing was not significantly altered (Figure 4B; Figure S3A). More importantly, Pq treatment did not decrease Tm-induced *gfp* mRNA expression (Figure 4C), indicating that iUPR^{ER} is blocked at a post-transcriptional stage by peroxide, possibly during translation, as reported earlier for peroxide stress (Shenton et al., 2006).

To confirm that the block is not specific for the construct used as the reporter, we used two GFP-tagged proteins that are upregulated upon Tm treatment (Figure 4D). Pq treatment was able to reduce the induction of these genes by Tm (Figure 4D), suggesting that the effect of ROS on iUPR^{ER} is not dependent on the specific reporter used for screening.

If endogenously generated peroxide is indeed responsible for abrogating red-iUPR^{ER} in the OQCΔ strains, it should mimic the features of translation downregulation observed with exogenous peroxide. Indeed, during red-iUPR^{ER}, OQCΔ strains showed a lower GFP protein level with unaffected Hac1 splicing and enhanced *gfp* mRNA expression in comparison with the WT, indicating that the decrease in red-iUPR^{ER} was at the level of translation (Figures 4E and 4F; Figure S2C). Subsequently, we demonstrated that the lower level of GFP in OQCΔ was not due to an enhanced degradation rate (Figure S3B; Supplemental Experimental Procedures). Next, we quantified the mRNA levels of validated UPR^{ER} reporters as a function of time after DTT treatment, and, as expected, transcripts typically induced by DTT in WT were also induced in OQCΔ strains with similar kinetics (Figure 4G). However, DTT-induced upregulation of Kar2 protein, a canonical reporter of iUPR^{ER}, was significantly reduced in *skn7Δ* strains at all time points during red-UPR^{ER} (Figures 4H and 4I; Figure S3C). Cycloheximide (CHX) chase experiments with Kar2 in the WT and *skn7Δ* strain confirmed that the enhanced ER-associated degradation (ERAD)-dependent degradation of Kar2 in *skn7Δ* was not responsible for the downregulation of Kar2 during reductive stress (Figure 4I; Figure S3D). Translation alteration was further confirmed by polysome profiles that clearly indicate that, upon DTT treatment of *skn7Δ* and *yap1Δ* cells, there was an increase in the monosome fraction at the cost of polysomes compared with the WT (Figure 4J; Figure S3E). This strongly suggests that red-iUPR^{ER} in OQCΔ strains is indeed affected through a translational block, as seen with Pq treatment.

In higher eukaryotes, eIF2α phosphorylation by PERK is a well known mechanism that couples ER stress to translation attenuation (Harding et al., 2000). Although PERK is absent in *S. cerevisiae*, we investigated whether the peroxide-mediated translation arrest is routed through either Gcn2, an eIF2α kinase (Dever et al., 1992), or Sch9, an S6-kinase homolog that is involved in regulating translation through the TOR pathway (Urban et al., 2007). Neither *gcn2* deletion nor a constitutively active mutant of Sch9 (c-sch9) (Urban et al., 2007) in the OQCΔ strains restored red-iUPR^{ER} amplitude (Figure 4K). Furthermore, these mutations failed to revert the attenuation of Tm-iUPR^{ER} in the presence of peroxide (Figure S3F). Ribosomal proteins tagged with GFP showed a similar trend in *skn7Δ* and WT cells during red-UPR^{ER} (Figure S3G) or when oxidative stress was coupled with iUPR^{ER} (Figure S3H), suggesting a mode of translation control independent of ribosomal concentration. Additionally, we did not find any increase in ribosomal aggregation in *skn7Δ* over WT cells during red-iUPR^{ER} (Figure S3I), which had been suggested as a major reason for translation downregulation in the *trx2Δ* strain (Glover-Cutter et al., 2013; Rand and Grant, 2006). Taken together, exogenous addition or endogenous peroxide accumulation arising because of failure of the OQC machinery can block iUPR^{ER} through downregulated translation that is independent of the canonical pathways routed through eIF2α, S6-kinase, ribosomal expression, or ribosome aggregation.

Oxidative Quality Control Regulates the Response to ER Stress in *C. elegans*

Can oxidative quality control pathways play a similar non-transcriptional role in metazoans that have a more complex UPR^{ER} pathway? We found that, consistent with the results obtained in *S. cerevisiae*, the presence of Pq significantly abrogated iUPR^{ER} in *C. elegans*, indicating the existence of a conserved mechanism in higher eukaryotes (Figure 5A; Experimental Procedures). RNAi-mediated knockdown of *skn-1*, a functional homolog of yeast *skn7* (An and Blackwell, 2003), led to a decrease in both Tm- and DTT-induced UPR^{ER} amplitude on the third day of adulthood (Figure 5B; Figure S4A) (all further experiments were performed on the third day of adulthood unless specifically mentioned otherwise). Unlike *S. cerevisiae*, higher eukaryotes are known to produce ROS during Tm-induced ER stress (Han et al., 2013; Harding et al., 2003), and we also detected significant ROS production in *C. elegans* after Tm treatment (Figure S4B; Harding et al., 2003). However, it is important to note that production of ROS during a non-reductive ER stress such as Tm can be mimicked in yeast by artificially increasing the disulfide load in the ER while suppressing ERAD (Haynes et al., 2004). This suggests a role of disulfide load in ROS production during ER stress. To enhance the generality of our finding

(D) Tm-induced changes in protein expression monitored in GFP-tagged strains in the presence or absence of Pq.
(E) *Hac1* splicing monitored in WT and OQCΔ strains upon treatment with 5 mM DTT for 3 hr. Marker lane is marked as M.
(F) qRT-PCR to measure *gfp* transcript levels in WT and OQCΔ strains upon treatment with 5 mM DTT for 3 hr.
(G) Canonical iUPR^{ER} transcripts were quantitated by qRT-PCR in WT and OQCΔ strains upon treatment with 5 mM DTT as a function of treatment time. All data were normalized to *ipp2* as the internal control.
(H) Treatment time-dependent immunoblot for Kar2p in the WT and a representative OQCΔ strain treated with 5 mM DTT. Quantification is shown at the bottom.
(I) Densitometric quantitation of time kinetics for Kar2 protein immunoblot done by cycloheximide pulse-chase treatment along with 5 mM DTT to measure the protein degradation rate in the WT and skn7Δ.
(J) Polysome profiling for skn7Δ and WT cells upon treatment with 5 mM DTT for 3 hr.
(K) iUPR^{ER} was measured in WT or OQCΔ strains that harbored either an additional deletion of *gcn2* or a constitutively active mutant of *sch9* (c-sch9). The cells were treated with 5 mM DTT for 3 hr.
See also Figure S3.

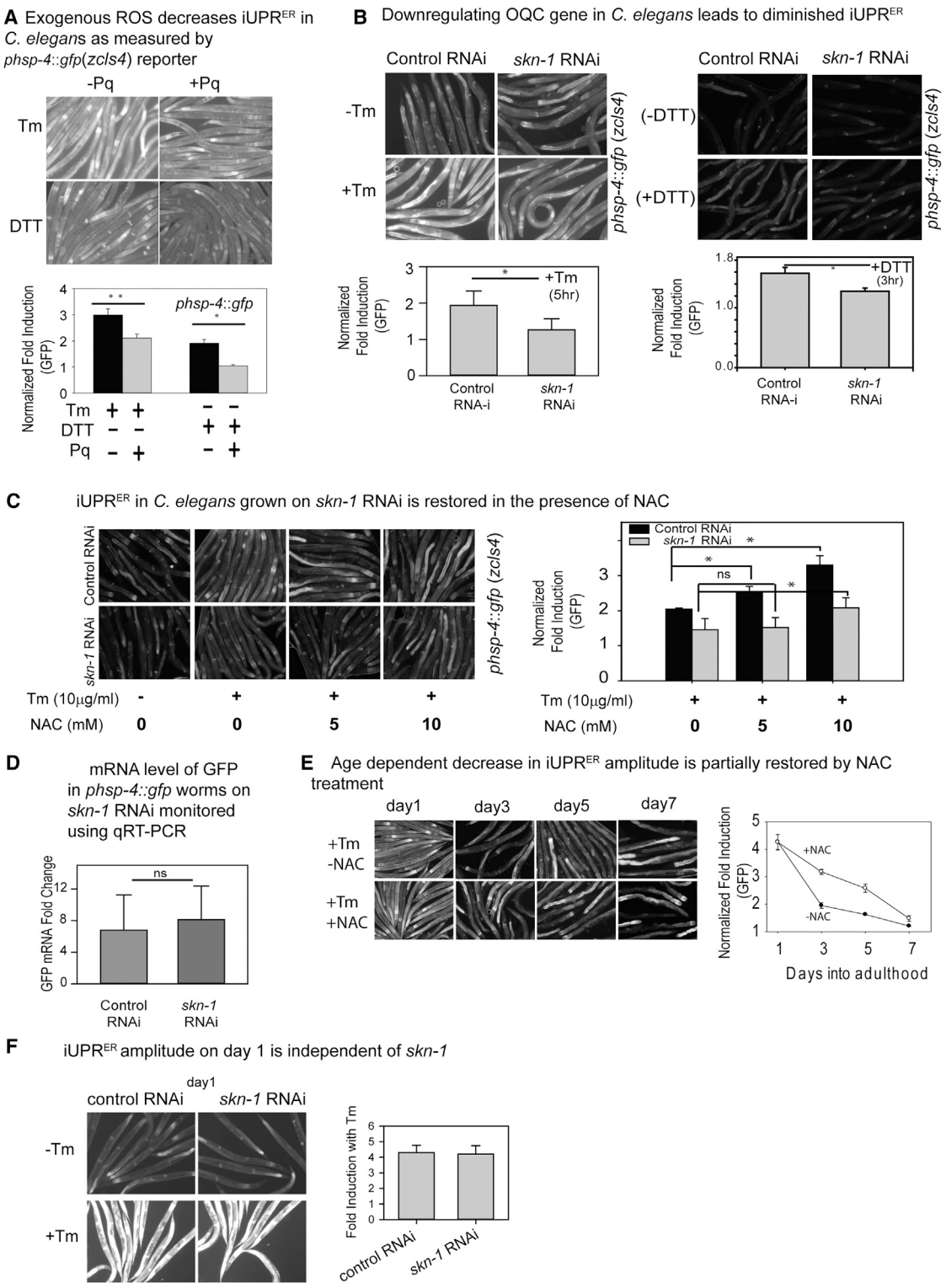

Figure 5. Oxidative Quality Control during ER Stress in *C. elegans*

(A) Epifluorescence images of day 1 adult *C. elegans* harboring an integrated *Phsp4::gfp* treated with 10 μg/ml Tm (top images) or 3 mM DTT (bottom images) in the absence or presence of 40 mM Pq for 8 hr. Densitometric quantitation of the data from three independent experiments is shown at the bottom.

(B) UPR^{ER} measured in *Phsp4::gfp* day 3 adult worms grown either on control or *skn-1* RNAi and treated with 10 μg/ml Tm or 3 mM DTT for the indicated time. Densitometric quantitation of the data is shown below.

(legend continued on next page)

encompassing ER stresses from different proteostasis perturbations in higher eukaryotes, we chose to work with Tm-iUPR^{ER} to elucidate the mechanism of OQC dependence in *C. elegans*.

Consistent with yeast data, the ROS scavenger N-acetylcysteine (NAC) was able to restore iUPR^{ER} amplitude in *skn-1* knockdown worms (Figure 5C), indicating that this supplementation is able to counteract the loss of OQC. Notably, the WT exhibits a higher increase in Tm-iUPR^{ER} in the presence of lower doses of NAC than *skn-1* downregulated worms (Figure 5C). This indicates that ROS accumulation upon Tm treatment is more in *skn-1* RNAi worms than in the WT. Although these observations do not exclude a role of *skn-1* in regulating the transcription of other genes during UPR^{ER} (Glover-Cutter et al., 2013), it does suggest that *skn-1* is required to scavenge ROS generated during ER stress, revealing a conserved mode of ROS-mediated regulation of UPR^{ER}.

We next investigated the conservation of ROS-mediated downregulation of iUPR^{ER} through translation control in *C. elegans*. Indeed, although downregulation of UPR^{ER}-induced *phsp4::gfp* was apparent at the protein level upon knockdown of *skn-1*, there was no significant reduction in the level of *gfp* mRNA (Figure 5D). This supports the results obtained from yeast and suggests a conserved mechanism of translation attenuation upon accumulation of ROS.

Next, to test whether ROS from other physiological sources can affect the amplitude of UPR^{ER} in worms, we took advantage of the fact that *C. elegans* is known to exhibit a burst in oxidative stress in the early stages of adulthood (Knoefler et al., 2012). We quantified iUPR^{ER} output as a function of age in the presence or absence of the anti-oxidant NAC. Indeed, we observed a partial rescue of iUPR^{ER} amplitude until the fifth day of adulthood(Figure 5E; Figure S4C), and the rescue was more significant during early adulthood, a period that coincides with an oxidative burst (Knoefler et al., 2012). Coherently, iUPR^{ER} during the first day of adulthood was less dependent on *skn-1* than on the third day (Figures 5B and 5F). Summarily, the crosstalk between ROS and iUPR^{ER} partially explains the loss of iUPR^{ER} amplitude with age. This, taken together with the fact that other sources of ROS like Pq, can affect iUPR^{ER}, emphasizes the importance of this crosstalk in shaping the amplitude of iUPR^{ER} in a large number of pathological conditions that exhibit hallmarks of increased intracellular oxidative stress.

Global Downregulation of iUPR^{ER} in Yeast through Bipartite Translation Control

Is there a global downregulation of red-UPR^{ER}-dependent protein expression in yeast upon deletion of *skn7Δ*? To answer this, we performed iTRAQ (isobaric tags for relative and absolute quantification)-based relative quantitative proteomics of stressed or unstressed WT and *skn7Δ* cells (Table S4). Proteins upregulated during red-iUPR^{ER} in WT cells were significantly less upregulated in *skn7Δ* during reductive stress. This confirmed a global downregulation of UPR^{ER} at the protein level in the absence of functional OQC. To factor in transcriptional program-dependent alterations, we quantified the transcriptional upregulation of the WT and *skn7Δ* during red-iUPR^{ER} using a microarray platform and obtained the correlation between relative induction of mRNAs and of their corresponding protein products. Interestingly, the correlation between mRNA and protein induction was higher in the WT than in *skn7Δ*. Although 38% of the protein variation could be predicted by altered mRNA expression in the WT, only 17% of the variation could be similarly explained in *skn7Δ* (Figure 6A), suggesting a loss of correlation between transcription and translation in *skn7Δ* during red-iUPR^{ER}. Additionally, the slope was lower for *skn7Δ* than the WT, indicating decreased translation of genes highly expressed during red-iUPR^{ER}, supporting the lower induction of iUPR^{ER} in *skn7Δ* relative to the WT.

Most importantly, although proteins upregulated by DTT in the WT were found to be less upregulated in deletion of *skn7Δ* (Figure 6B; Supplemental Notes), proteins that are repressed in WT cells during red-iUPR^{ER} are less repressed in *skn7Δ* (Figures S5A and S5B), suggesting a bipartite regulation of the protein expression level during iUPR^{ER} under OQC-deficient conditions.

Because we substantiated that the endogenous oxidative stress in OQCΔ strains leads to bipartite regulation of translation, we tested whether this holds true during oxidative stress. To eliminate the possibility of inherent bias of proteomics data toward highly abundant proteins, we performed a screen with ~900 GFP-tagged strains of yeast (Huh et al., 2003) in the presence of exogenous peroxide (Experimental Procedures). Indeed, in spite of the general downregulation at the protein level, the bipartite nature of protein expression became more apparent. Highly expressed ones were prone to downregulation in the presence of peroxide, whereas proteins that were expressed at a lower level were upregulated (Figure 6C; Figure S5C; Supplemental Notes for Figure 6C; Table S3). Thus, regulation with peroxide shows a unique bipartite control of protein expression levels distinct from canonical translational regulation, leading to global abrogation of protein expression.

This observation led us to investigate the underlying mechanism in translation control during reductive stress. Recent reports suggest the role of codon usage in regulating the translation of stress response proteins (Begley et al., 2007; Chan et al., 2015; Endres et al., 2015). Analysis of the codon usage revealed that even the optimal codons for the same amino acids are not used similarly by the abundant and non-abundant proteins (Figure 6D). As an example, the TTC codon of phenylalanine is used more in the abundant proteins than the non-abundant

(C) Epifluorescence images of *Phsp4::gfp* worms on control and *skn-1* RNAi treated with a combination of 10 μg/ml Tm and increasing concentrations of NAC. Densitometric quantitation of the data is shown at the left.
(D) qRT-PCR to measure the fold change in *gfp* mRNA level in *Phsp-4::gfp* worms treated with control RNAi or *skn-1* RNAi in the presence of 10 μg/ml Tm for 5 hr.
(E) Epifluorescence images of *Phsp-4::gfp* worms on different days of adulthood when treated with 10 μg/ml Tm in the absence or presence of 10 mM NAC. Right: average of the normalized fold induction of GFP.
(F) Epifluorescence images of 1-day-old adult *Phsp4::gfp* worms on control RNAi or *skn-1* RNAi treated with 10 μg/ml of Tm for 5 hr. Densitometric quantification is shown at the right.
For all samples, *$p < 0.05$ and **$p < 0.005$, with two-tailed Student's t test on a minimum of three replicates. ns, non-significant. See also Figure S4.

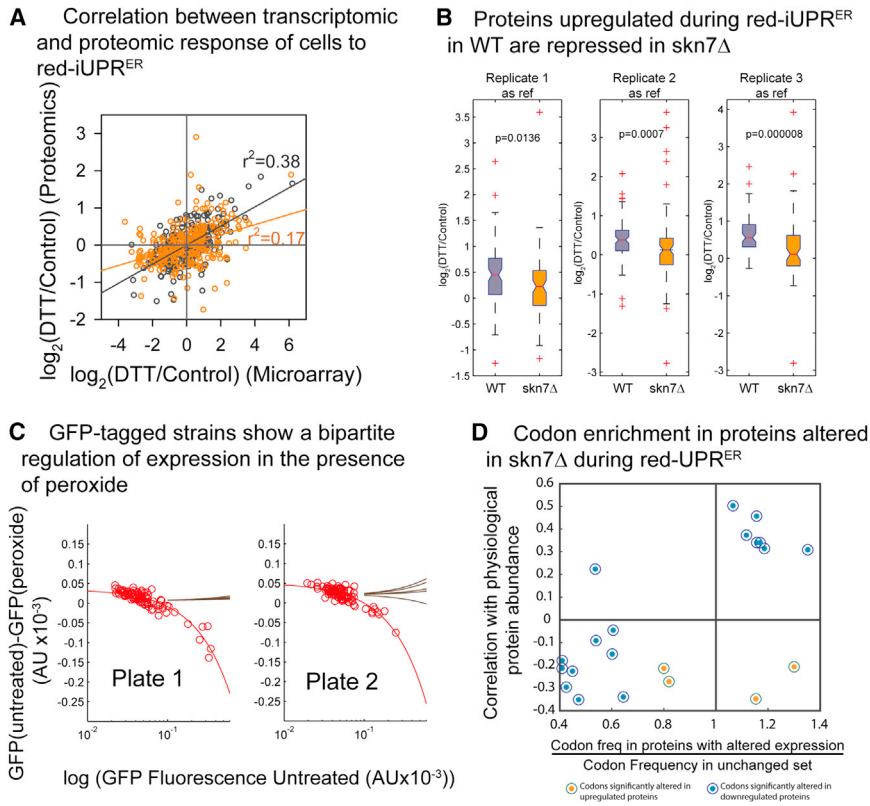

Figure 6. Unmitigated Oxidative Stress Leads to a Non-canonical Bipartite Regulation of Protein Expression

(A) Quantitative proteomics using iTRAQ were used to measure the proteome-wide alteration in protein level in WT and skn7Δ strains during red-iUPR^{ER}. A microarray was used to measure the alteration in mRNA abundance under similar conditions. Fold upregulation of protein expression during red-iUPR^{ER} is plotted against fold upregulation of mRNA during the same stress in WT and skn7Δ.

(B) Proteins that are upregulated in the WT because of red-UPR^{ER} (WT(+DTT)/WT > 1.2) in one replicate were taken, and the average ratio of (SKN7Δ+DTT)/SKN7Δ or (WT+DTT)/WT was calculated for these proteins for the other two replicates. This has been done in turn by taking the first (left), second (center), or third (right) replicate as reference and plotting as a boxplot.

(C) A GFP-tagged gene collection was used to obtain single-cell fluorescence for each of the strains in the absence and presence of 5 mM peroxide (two representative plates are shown). The difference in protein expression (difference in GFP fluorescence) is plotted against GFP fluorescence in untreated samples for all plates independently. Linear regression of the data is shown as a red line. Ten representative regressions obtained upon data shuffling are shown in black to show the significance of the original regression line. The blue line shows the reference for unchanged expression level upon treatment. See also Figure S5C.

(D) Codon frequency analyses were carried out for proteins that were either upregulated or downregulated in skn7Δ during red-UPR^{ER}. Only the codons that showed a statistically significant difference ($p < 0.1$, Mann-Whitney rank correlation) with the control set are shown in the plot. The enrichment of the codon frequency in the test set with respect to the control set is plotted on the x axis, whereas the correlation of the same codon with respect to protein abundance is plotted on the y axis.

See also Supplemental Notes for this figure, Figures S5 and S6, and Tables S3 and S4.

ones, whereas the opposite is true for the TTT codon. Similar patterns are seen across multiple different amino acids. Using this, we asked whether the proteins that are translationally downregulated in *skn7Δ* during red-UPR^{ER} show a different codon usage pattern than the ones that are upregulated. Indeed, many of the codons that show a strong positive correlation with abundance were enriched in the former set, whereas the ones that show a negative correlation with abundance were depleted (Figure S6A), indicating that altered codon usage may allow the downregulation of more abundant proteins while increasing the expression of less abundant ones.

Thus, unchecked oxidative stress during reductive ER stress leads to a collapse of the UPR^{ER} program by partial uncoupling of protein expression from transcriptional alterations. This is primarily affected by an uncoordinated regulation of translation that acts in a bipartite manner to decrease protein expression of upregulated genes while increasing the expression of the repressed ones.

Activation of PERK Decreases ROS Formation during ER Stress

Does ROS-dependent uncoordinated translation deregulation cross-talk with the UPR-dependent and PERK-mediated translation attenuation? PERK, a translation attenuator in higher eukaryotes, is implicated in ROS clearance (Avezov et al., 2013; Cullinan and Diehl, 2004). We also observed a significant increase in oxidative damage in the *C. elegans* PERK deletion strain *pek-1(ok275)* (Figure 7A). Additionally, the expression of *gst-4*, a canonical anti-oxidative stress response gene, was found to be induced in a PERK deletion strain, *pek-1(ok275)* (Figure 7B), indicative of an elevated level of oxidative stress upon PERK deletion. These observations suggest that PERK-dependent mechanisms may resolve ROS-dependent translation deregulation. Accordingly, PERK inactivation would downregulate the amplitude of iUPR^{ER}. This is indeed the case; Tm-induced expression of *phsp4::gfp* reporter was muffled in *pek-1(ok275)* (Figure 7C). The response was recovered in the mutant strain upon treatment with NAC (Figure 7D), confirming that this branch plays an important role in reducing ROS formation. Thus, paradoxically, PERK, the translation attenuation machinery, prevents ROS-mediated translation arrest and helps in maintaining iUPR^{ER} signaling through other branches. Because PERK activation leads to the loss of canonical translation and, hence, to a lower load of protein in the ER, it is difficult to uncouple the antioxidant activity of the downstream genes from the benefits of translation inhibition brought about by PERK. We

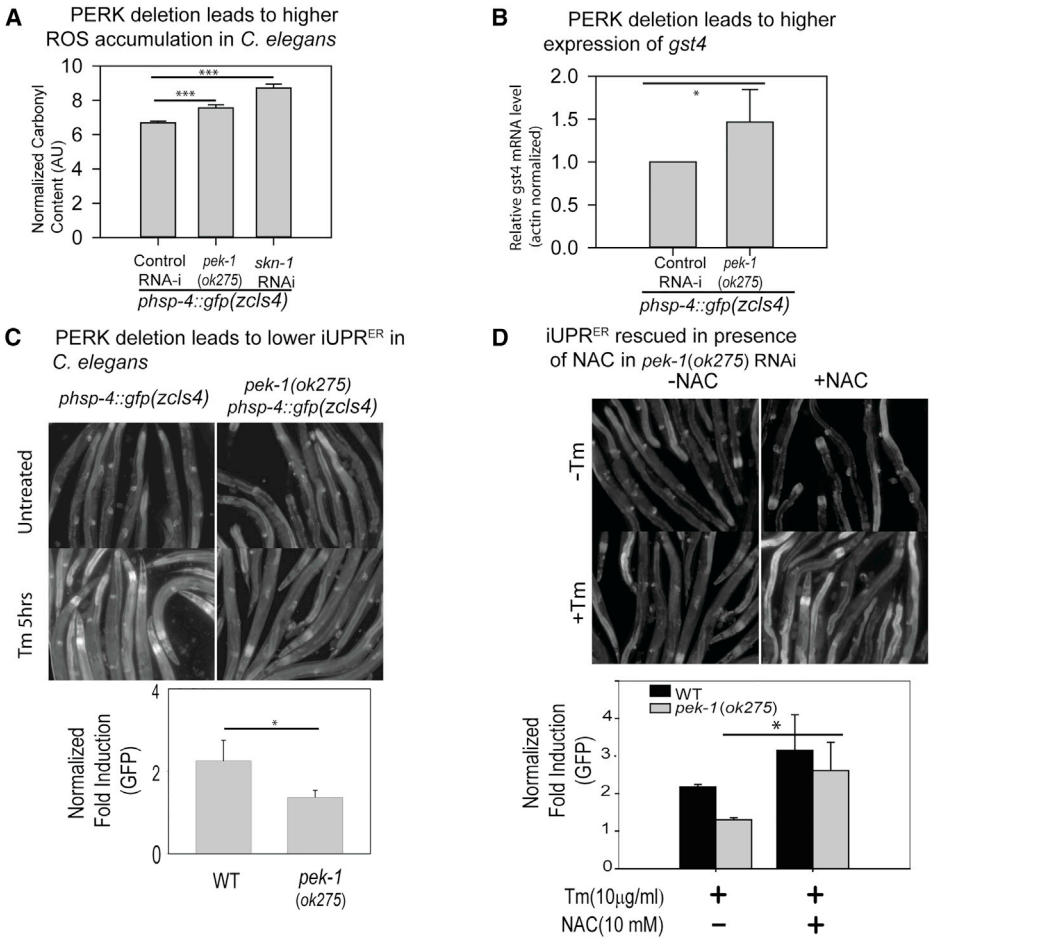

(legend on next page)

took advantage of *S. cerevisiae* because it lacks a PERK homolog. We reasoned that decreasing general translation in yeast, using an orthogonal system, would reduce the overall concentration of proteins in the ER and thereby diminish the load on the disulfide exchange systems. This should reduce ROS during reductive stress and, hence, decrease the OQC dependence of red-iUPR^{ER}. We used sublethal concentrations of the antibiotics nourseothricin (CloNAT) and hygromycin (Hyg), both well known inhibitors of eukaryotic protein synthesis, to downregulate translation. As expected, pre-treatment of *S. cerevisiae* with these antibiotics, which act as translation inhibitors, decreased iUPR^{ER} in a dose-dependent manner in the WT strain (Figure S7A). However, at antibiotics concentrations where iUPR^{ER} is downregulated, the difference between the WT and OQCΔ strains is marginal, unlike the large difference observed in the absence of these antibiotics (Figures 7E and 7F). As a control, Tm-iUPR^{ER} decreased similarly in both the WT and OQCΔ strains as a function of CloNAT concentration (Figure S7B), highlighting the importance of translation attenuation specifically during ROS-producing ER stress. Similar results were obtained when translation was attenuated by decreasing glucose concentration in the medium (Figure 7G). This attests to the fact that repressing protein translation may decrease ROS production. Consistent with this idea, treatment with CloNAT decreased DTT-induced ROS production in the OQCΔ strains (Figure 7H). If reduction in translation is important in limiting electron transfer to oxygen, then a decrease in ROS production and not enhanced clearance should be evident in the presence of translation inhibitors. Consistently, an Oxyplate assay confirmed that the burst in oxygen consumption, induced during reductive stress, decreases in the presence of the translation inhibitor CloNAT in a concentration-dependent manner (Figure 7I; Figure S7C). Thus, an orthogonal translation attenuation system is able to decrease ROS production and decrease the dependence of UPR^{ER} on oxidative stress response pathways in yeast.

Summarizing the results from *C. elegans* and yeast, it may be concluded that PERK-dependent translation attenuation is able to decrease ROS through either direct activation of the antioxidant response or through a decrease in protein translation. This suggests that a more regulated translation attenuation system is able to counter ROS-dependent dysregulation of protein expression during UPR^{ER}.

DISCUSSION

We discovered a previously uncharacterized relationship between UPR^{ER} and a ROS-mediated non-canonical mode of translation deregulation during reductive stress. It is generally believed that reductive stress would not initiate an antagonistic oxidative stress based on the premise that oxidative free radicals would be unstable in the presence of a reducing agent (Glover-Cutter et al., 2013; Rand and Grant, 2006). Here we uncover a seemingly contradicting mechanism by which ROS-mediated translation attenuation compromises the ER stress response to reducing agents, decreasing cellular tolerance to reductive stress. However, we show that this mechanism is part of an intricate feedback loop for the downregulation of the ER stress response. This also buffers the subsequent ROS production, enabling the cells to maintain homeostasis. In support of this mechanism, we find that PERK, a central regulator of the ER stress response, may have evolved to limit oxidative stress in cells that are burdened with oxidative folding in the ER. Furthermore, we demonstrate a type of bipartite translation attenuation that could represent a mode of signaling process.

The results of this study have three major implications. First, oxidative stress response pathways may play a key role in maintaining ER homeostasis in cells that are burdened with a high disulfide load. Cells like pancreatic acinar cells and B cells (Shimizu and Hendershot, 2009) are burdened with a high disulfide load because of the nature of their secretome. Because oxygen typically acts as the terminal electron acceptor for oxidative folding (Koritzinsky et al., 2013), a high disulfide load would correspondingly produce high amounts of reactive oxygen species. Our study implicates that these cells would be sensitive to impaired ROS clearance mechanisms or ROS generation from other sources because the ER stress response pathways would be blocked in the presence of unchecked ROS accumulation. This is consistent with other studies that have hinted at the importance of anti-oxidative agents in assisting protein secretion (Malhotra et al., 2008). Importantly, oxidative stress response pathways mediated by skn-1 are known to be required for a healthy lifespan (Tullet et al., 2008), and its homolog NRF2 is also a known regulator for healthy aging (Lewis et al., 2010). Our study highlights an additional importance of these pathways

Figure 7. Orthogonal Translation Control Reduces ROS during UPR^{ER} and Decreases the Dependence on OQC

(A) The concentrations of protein carbonyl groups were measured using the DNPH alkaline method in WT, *pek-1* knockout (KO), and *skn-1* knockdown (KD) worms on day 3.

(B) qRT-PCR to measure the GST4 mRNA level in *Phsp4::gfp(zcls4)* grown on control RNAi and *skn-1* RNAi.

(C) iUPR^{ER} was measured following 5 hr of Tm treatment in *Phsp4::gfp(zcls4)* and *pek-1(ok275)Phsp4::gfp(zcls4)* strains on day 3 of adulthood. Normalized GFP fold induction was quantified from fluorescence images (bottom).

(D) iUPR^{ER} was measured after treatment of *pek-1(ok275)Phsp4::gfp(zcls4)* worms with or without 10 mM NAC in the absence or presence of 10 μg/ml Tm. Bottom: quantification.

(E–G) iUPR^{ER} was measured in WT and OQCΔ strains of *S. cerevisiae* (using the UPRE::GFP reporter) while they were maintained on different concentrations of CloNAT (E), hygromycin (F), or glucose (G) and treated with 5 mM DTT. The data plotted are normalized to the response of the WT strain at concentration of antibiotics or glucose.

(H) Representative flow cytometry histograms of DHR123 staining of *yap1Δ* (left) and *skn7Δ* (right) strains upon treatment with 5 mM DTT in the presence or absence of 200 nM CloNAT.

(I) 5 mM DTT-induced oxygen consumption was monitored in the presence of different concentrations of CloNAT in WT cells.

For all samples, *$p < 0.05$ with two-tailed Student's t test on a minimum of three replicates.

See also Figure S7.

in maintaining protein homeostasis during progressive aging, primarily in the context of secretory cells.

Second, uncontrolled accumulation of ROS may uncouple the transcript-level and proteome-level response of a cell to ER stress. Our study provides, as a maiden report, different dynamics of gene and protein expression that lead to loss of correlation between the response and phenotype through a novel ROS-regulated mode of translation regulation that is independent of the known canonical models. We implicate codon usage to play an important role in this mode of regulation, whereby the expression of abundant proteins is suppressed whereas the less abundant ones are enriched in the proteome. This adds to the growing literature of how altered codon usage pattern may shape the cellular response to stress (Begley et al., 2007; Chan et al., 2015; Endres et al., 2015).

Third, PERK, an effector of canonical translation attenuation, may have evolved to mitigate the translation deregulation by ROS. This, we speculate, has allowed the evolution of disulfide-enriched proteomes. Through our studies, we show how PERK prevents the more catastrophic bipartite regulation by ROS by either directly allowing expression of anti-oxidative genes or by decreasing the protein load in the ER through a well regulated mechanism (Cullinan and Diehl, 2004; Harding et al., 2000). This, in conjunction with its demonstrated anti-oxidative role, highlights its importance in coupling ER stress to translation attenuation and implicates it in enabling cells to handle high ROS, which is linked to a high disulfide burden.

Collectively, a simple mechanism of peroxide-mediated translation attenuation and modulation of UPR^{ER} may have far-reaching implications in pathophysiological conditions that are linked to elevated ROS (Hekimi et al., 2011; Reczek and Chandel, 2015). Importantly, this integration leads to alteration of translation, a phenomenon that is undetectable at the level of transcripts. It will now be important to unravel the alteration of UPR^{ER} at the proteome level to delineate the detailed mechanism of peroxide-mediated signal integration.

EXPERIMENTAL PROCEDURES

Yeast Screening and Biochemical Experiments

A synthetic genetic array strategy (Tong et al., 2001) was used to cross each strain containing a loss-of-function allele (~6,000 strains in total) with the reporter strain (ymj003) to make the library of haploid strains carrying the reporter and loss-of-function allele. All cells were grown in yeast extract peptone dextrose (YPD) (1% yeast extract, 2% peptone, and 2% glucose) in the presence of G418 for the initial screening. For all fluorescence-activated cell sorting (FACS)-based fluorescence assays, yeast cells were grown for 3 hr to reach optical density 600 (OD_{600}) of 0.4–0.6 and then treated with 5 mM DTT for 3 hr, followed by measuring the GFP and RFP fluorescence using a flow cytometer. The same treatment regimes, along with published protocols, were followed for polysome profiling (Baim et al., 1985), microarray (Agilent platform), proteomics (iTRAQ), immunoblotting, and qRT-PCR experiments. All treatments for screening purpose were done in 96-well assay plates. The median fluorescence values of GFP and RFP were extracted, and analyses were carried out using in-house scripts. For experiments with GFP-tagged yeast strains in peroxide, the cells were grown until log phase and then treated with 1 mM H_2O_2 for 3 hr. Fluorescence of GFP was measured using flow cytometry.

Oxyplate Assay and ROS Measurement

The yeast cells were grown on synthetic dextrose medium with 100 mM (4-(2-hydroxyethyl)-1-peperazineethanesulfonic acid (HEPES) (pH 7) for 3 hr, transferred to BD Oxyplates, and treated as discussed in the experiments. Fluorescence kinetics were measured using a Tecan multimode reader (excitation 480 nm/emission 620 nm) according to the manufacturer's instructions. For ROS measurements using DHR123 and DHE, cells were grown in YPD until log phase and treated with 5 mM DTT for 3 hr or 5 μg/ml Tm for 4 hr, and then ROS-specific dyes were added and incubated for 12 min. After washing off the excess dye, fluorescence was measured using FACS.

C. elegans Strains and Maintenance

Strains were cultured at 20°C on NGM plates seeded with OP50. The strains used in this study were N2 Bristol wild-type, *pek-1(ok275)*, *Phsp-4:gfp(zcIs4)*, and *pek-1(ok275); Phsp-4:gfp(zcIs4)*.

C. elegans UPR^{ER} Reporter Assays

Phsp-4:gfp(zcIs4) or *pek-1(ok275); Phsp-4:gfp(zcIs4)* worms were bleached, and eggs were placed on nematode growth medium (NGM) plates seeded with control (empty pL4440 vector) or *skn-1* RNAi plates. Day 3 adult worms were treated with 10 μg/ml Tm or 3 mM DTT for the indicated time, and GFP fluorescence was quantified. For Pq and Tm/DTT double treatment experiments, day 1 adults grown on control RNAi were processed for fluorescence microscopy. For ROS scavenging experiments, worms on different days of adulthood were supplemented with 10 mM NAC along with Tm (for 5 hr), and then UPR^{ER} was measured. A colorimetric carbonylation assay was performed from lysates directly using dinitro phenyl hydrazine (DNPH) reaction and absorbance or by blotting with anti-DNPH antibodies.

Statistical Methods

Statistical analyses were conducted using Student's t test and paired Student's t test with Sigma Plot.

ACCESSION NUMBERS

The accession number for the microarray data reported in this paper is GEO: GSE68006.

SUPPLEMENTAL INFORMATION

Supplemental Information includes Supplemental Experimental Procedures, seven figures, and six tables and can be found with this article online at http://dx.doi.org/10.1016/j.celrep.2016.06.025.

AUTHOR CONTRIBUTIONS

S.M., A.R., A.B., A.G., G.A., S.K., and N.R.B. contributed to the generation of reagents related to yeast and validation of the screening process. L.M. contributed to the generation of reagents in *C. elegans* and experiments with *C. elegans*. S.M., A.R., A.B., and A.G. were involved in the screening process and other yeast experiments. S.M. and A.B. were involved in the proteomics experiments. S.M., A.R., and A.G. were involved in the microarray experiments. S.M., A.R., L.M., A.G., A.B., S.S.G., A.M., and K.C. wrote the manuscript, and all authors critically reviewed it. K.C., A.M., and S.S.G. supervised the work. K.C. conceived the project, and K.C. and S.M. were instrumental in standardizing all preliminary screens and procedures.

ACKNOWLEDGMENTS

K.C. is a Wellcome Trust-DBT India Alliance (IA) Intermediate Fellow, and this project was majorly funded by the IA. S.M. and A.R. acknowledge CSIR for graduate fellowships. L.M., A.G., and N.R.B. acknowledge UGC for fellowship support. G.A. and S.K. acknowledge the IA for fellowship support. A.M. acknowledges DBT and NII for infrastructural and funding support. We thank Dr. Kaustuv Dutta and Vignesh Kumar for their help with polysome profiling experiments. We thank the members of the K.C. lab for critically reviewing the manuscript. We thank Jonathan Weissman for the generous gift of the *S. cerevisiae* strain harboring the UPR^{ER} reporter construct.

Received: July 16, 2015
Revised: April 11, 2016
Accepted: June 3, 2016
Published: June 30, 2016

REFERENCES

An, J.H., and Blackwell, T.K. (2003). SKN-1 links C. elegans mesendodermal specification to a conserved oxidative stress response. Genes Dev. *17*, 1882–1893.

Avery, A.M., and Avery, S.V. (2001). Saccharomyces cerevisiae expresses three phospholipid hydroperoxide glutathione peroxidases. J. Biol. Chem. *276*, 33730–33735.

Avezov, E., Cross, B.C., Kaminski Schierle, G.S., Winters, M., Harding, H.P., Melo, E.P., Kaminski, C.F., and Ron, D. (2013). Lifetime imaging of a fluorescent protein sensor reveals surprising stability of ER thiol redox. J. Cell Biol. *201*, 337–349.

Back, S.H., and Kaufman, R.J. (2012). Endoplasmic reticulum stress and type 2 diabetes. Annu. Rev. Biochem. *81*, 767–793.

Baim, S.B., Pietras, D.F., Eustice, D.C., and Sherman, F. (1985). A mutation allowing an mRNA secondary structure diminishes translation of Saccharomyces cerevisiae iso-1-cytochrome c. Mol. Cell. Biol. *5*, 1839–1846.

Begley, U., Dyavaiah, M., Patil, A., Rooney, J.P., DiRenzo, D., Young, C.M., Conklin, D.S., Zitomer, R.S., and Begley, T.J. (2007). Trm9-catalyzed tRNA modifications link translation to the DNA damage response. Mol. Cell *28*, 860–870.

Brandman, O., Stewart-Ornstein, J., Wong, D., Larson, A., Williams, C.C., Li, G.W., Zhou, S., King, D., Shen, P.S., Weibezahn, J., et al. (2012). A ribosome-bound quality control complex triggers degradation of nascent peptides and signals translation stress. Cell *151*, 1042–1054.

Breslow, D.K., Cameron, D.M., Collins, S.R., Schuldiner, M., Stewart-Ornstein, J., Newman, H.W., Braun, S., Madhani, H.D., Krogan, N.J., and Weissman, J.S. (2008). A comprehensive strategy enabling high-resolution functional analysis of the yeast genome. Nat. Methods *5*, 711–718.

Cao, S.S., and Kaufman, R.J. (2012). Unfolded protein response. Curr. Biol. *22*, R622–R626.

Chan, C.T., Deng, W., Li, F., DeMott, M.S., Babu, I.R., Begley, T.J., and Dedon, P.C. (2015). Highly Predictive Reprogramming of tRNA Modifications Is Linked to Selective Expression of Codon-Biased Genes. Chem. Res. Toxicol. *28*, 978–988.

Cullinan, S.B., and Diehl, J.A. (2004). PERK-dependent activation of Nrf2 contributes to redox homeostasis and cell survival following endoplasmic reticulum stress. J. Biol. Chem. *279*, 20108–20117.

Dever, T.E., Feng, L., Wek, R.C., Cigan, A.M., Donahue, T.F., and Hinnebusch, A.G. (1992). Phosphorylation of initiation factor 2 alpha by protein kinase GCN2 mediates gene-specific translational control of GCN4 in yeast. Cell *68*, 585–596.

Endres, L., Dedon, P.C., and Begley, T.J. (2015). Codon-biased translation can be regulated by wobble-base tRNA modification systems during cellular stress responses. RNA Biol. *12*, 603–614.

Gasch, A.P., Spellman, P.T., Kao, C.M., Carmel-Harel, O., Eisen, M.B., Storz, G., Botstein, D., and Brown, P.O. (2000). Genomic expression programs in the response of yeast cells to environmental changes. Mol. Biol. Cell *11*, 4241–4257.

Glover-Cutter, K.M., Lin, S., and Blackwell, T.K. (2013). Integration of the unfolded protein and oxidative stress responses through SKN-1/Nrf. PLoS Genet. *9*, e1003701.

Han, J., Back, S.H., Hur, J., Lin, Y.H., Gildersleeve, R., Shan, J., Yuan, C.L., Krokowski, D., Wang, S., Hatzoglou, M., et al. (2013). ER-stress-induced transcriptional regulation increases protein synthesis leading to cell death. Nat. Cell Biol. *15*, 481–490.

Harding, H.P., Zhang, Y., Bertolotti, A., Zeng, H., and Ron, D. (2000). Perk is essential for translational regulation and cell survival during the unfolded protein response. Mol. Cell *5*, 897–904.

Harding, H.P., Zhang, Y., Zeng, H., Novoa, I., Lu, P.D., Calfon, M., Sadri, N., Yun, C., Popko, B., Paules, R., et al. (2003). An integrated stress response regulates amino acid metabolism and resistance to oxidative stress. Mol. Cell *11*, 619–633.

Haynes, C.M., Titus, E.A., and Cooper, A.A. (2004). Degradation of misfolded proteins prevents ER-derived oxidative stress and cell death. Mol. Cell *15*, 767–776.

Haze, K., Yoshida, H., Yanagi, H., Yura, T., and Mori, K. (1999). Mammalian transcription factor ATF6 is synthesized as a transmembrane protein and activated by proteolysis in response to endoplasmic reticulum stress. Mol. Biol. Cell *10*, 3787–3799.

Hekimi, S., Lapointe, J., and Wen, Y. (2011). Taking a "good" look at free radicals in the aging process. Trends Cell Biol. *21*, 569–576.

Henderson, L.M., and Chappell, J.B. (1993). Dihydrorhodamine 123: a fluorescent probe for superoxide generation? Eur. J. Biochem. *217*, 973–980.

Huh, W.K., Falvo, J.V., Gerke, L.C., Carroll, A.S., Howson, R.W., Weissman, J.S., and O'Shea, E.K. (2003). Global analysis of protein localization in budding yeast. Nature *425*, 686–691.

Jonikas, M.C., Collins, S.R., Denic, V., Oh, E., Quan, E.M., Schmid, V., Weibezahn, J., Schwappach, B., Walter, P., Weissman, J.S., and Schuldiner, M. (2009). Comprehensive characterization of genes required for protein folding in the endoplasmic reticulum. Science *323*, 1693–1697.

Knoefler, D., Thamsen, M., Koniczek, M., Niemuth, N.J., Diederich, A.K., and Jakob, U. (2012). Quantitative in vivo redox sensors uncover oxidative stress as an early event in life. Mol. Cell *47*, 767–776.

Koritzinsky, M., Levitin, F., van den Beucken, T., Rumantir, R.A., Harding, N.J., Chu, K.C., Boutros, P.C., Braakman, I., and Wouters, B.G. (2013). Two phases of disulfide bond formation have differing requirements for oxygen. J. Cell Biol. *203*, 615–627.

Lee, J., Godon, C., Lagniel, G., Spector, D., Garin, J., Labarre, J., and Toledano, M.B. (1999). Yap1 and Skn7 control two specialized oxidative stress response regulons in yeast. J. Biol. Chem. *274*, 16040–16046.

Lewis, K.N., Mele, J., Hayes, J.D., and Buffenstein, R. (2010). Nrf2, a guardian of healthspan and gatekeeper of species longevity. Integr. Comp. Biol. *50*, 829–843.

Malhotra, J.D., and Kaufman, R.J. (2007). Endoplasmic reticulum stress and oxidative stress: a vicious cycle or a double-edged sword? Antioxid. Redox Signal. *9*, 2277–2293.

Malhotra, J.D., Miao, H., Zhang, K., Wolfson, A., Pennathur, S., Pipe, S.W., and Kaufman, R.J. (2008). Antioxidants reduce endoplasmic reticulum stress and improve protein secretion. Proc. Natl. Acad. Sci. USA *105*, 18525–18530.

Mori, K., Sant, A., Kohno, K., Normington, K., Gething, M.J., and Sambrook, J.F. (1992). A 22 bp cis-acting element is necessary and sufficient for the induction of the yeast KAR2 (BiP) gene by unfolded proteins. EMBO J. *11*, 2583–2593.

Rand, J.D., and Grant, C.M. (2006). The thioredoxin system protects ribosomes against stress-induced aggregation. Mol. Biol. Cell *17*, 387–401.

Reczek, C.R., and Chandel, N.S. (2015). ROS-dependent signal transduction. Curr. Opin. Cell Biol. *33*, 8–13.

Ron, D., and Walter, P. (2007). Signal integration in the endoplasmic reticulum unfolded protein response. Nat. Rev. Mol. Cell Biol. *8*, 519–529.

Schwer, B., Sawaya, R., Ho, C.K., and Shuman, S. (2004). Portability and fidelity of RNA-repair systems. Proc. Natl. Acad. Sci. USA *101*, 2788–2793.

Shamu, C.E., and Walter, P. (1996). Oligomerization and phosphorylation of the Ire1p kinase during intracellular signaling from the endoplasmic reticulum to the nucleus. EMBO J. *15*, 3028–3039.

Shenton, D., Smirnova, J.B., Selley, J.N., Carroll, K., Hubbard, S.J., Pavitt, G.D., Ashe, M.P., and Grant, C.M. (2006). Global translational responses to oxidative stress impact upon multiple levels of protein synthesis. J. Biol. Chem. *281*, 29011–29021.

Shimizu, Y., and Hendershot, L.M. (2009). Oxidative folding: cellular strategies for dealing with the resultant equimolar production of reactive oxygen species. Antioxid. Redox Signal. *11*, 2317–2331.

Tarpey, M.M., and Fridovich, I. (2001). Methods of detection of vascular reactive species: nitric oxide, superoxide, hydrogen peroxide, and peroxynitrite. Circ. Res. *89*, 224–236.

Taylor, R.C., and Dillin, A. (2013). XBP-1 is a cell-nonautonomous regulator of stress resistance and longevity. Cell *153*, 1435–1447.

Temple, M.D., Perrone, G.G., and Dawes, I.W. (2005). Complex cellular responses to reactive oxygen species. Trends Cell Biol. *15*, 319–326.

Tirasophon, W., Welihinda, A.A., and Kaufman, R.J. (1998). A stress response pathway from the endoplasmic reticulum to the nucleus requires a novel bifunctional protein kinase/endoribonuclease (Ire1p) in mammalian cells. Genes Dev. *12*, 1812–1824.

Tong, A.H., Evangelista, M., Parsons, A.B., Xu, H., Bader, G.D., Pagé, N., Robinson, M., Raghibizadeh, S., Hogue, C.W., Bussey, H., et al. (2001). Systematic genetic analysis with ordered arrays of yeast deletion mutants. Science *294*, 2364–2368.

Travers, K.J., Patil, C.K., Wodicka, L., Lockhart, D.J., Weissman, J.S., and Walter, P. (2000). Functional and genomic analyses reveal an essential coordination between the unfolded protein response and ER-associated degradation. Cell *101*, 249–258.

Tullet, J.M., Hertweck, M., An, J.H., Baker, J., Hwang, J.Y., Liu, S., Oliveira, R.P., Baumeister, R., and Blackwell, T.K. (2008). Direct inhibition of the longevity-promoting factor SKN-1 by insulin-like signaling in C. elegans. Cell *132*, 1025–1038.

Urban, J., Soulard, A., Huber, A., Lippman, S., Mukhopadhyay, D., Deloche, O., Wanke, V., Anrather, D., Ammerer, G., Riezman, H., et al. (2007). Sch9 is a major target of TORC1 in Saccharomyces cerevisiae. Mol. Cell *26*, 663–674.

Walter, P., and Ron, D. (2011). The unfolded protein response: from stress pathway to homeostatic regulation. Science *334*, 1081–1086.

Winzeler, E.A., Shoemaker, D.D., Astromoff, A., Liang, H., Anderson, K., Andre, B., Bangham, R., Benito, R., Boeke, J.D., Bussey, H., et al. (1999). Functional characterization of the S. cerevisiae genome by gene deletion and parallel analysis. Science *285*, 901–906.